Available online at www.sciencedirect.com
ScienceDirect
Diamond & Related Materials 17 (2008) 325–335
DIAMOND AND RELATED MATERIALS
www.elsevier.com/locate/diamond

On the use of CrN/Cr and CrN interlayers in hot filament chemical vapour deposition (HF-CVD) of diamond films onto WC-Co substrates

Riccardo Polini [a], Massimiliano Barletta [b,*]

[a] Dipartimento di Scienze e Tecnologie Chimiche, Università di Roma Tor Vergata, Via della Ricerca Scientifica, 1, Rome, 00133, Italy
[b] Dipartimento di Ingegneria Meccanica, Università di Roma Tor Vergata, Via del Politecnico, 1, Rome, 00133, Italy

Received 25 July 2007; received in revised form 21 December 2007; accepted 31 December 2007
Available online 12 January 2008

Abstract

CrN/Cr-based films were deposited using PVD-arc technique onto Co-cemented tungsten carbide (WC-Co) substrates and, then, seeded with diamond powder suspension or mechanically treated by Fluidized Bed Peening (FBP) of brittle diamond powders. Multilayered coatings were obtained from the superimposition of 4 μm-thick diamond coatings, deposited on the PVD interlayer using hot filament chemical vapour deposition (HFCVD). The effectiveness of fluidized bed peened CrN/Cr interlayers on the adhesion enhancement of diamond on WC-Co substrates was studied and compared to diamond coated WC-Co substrates with unpeened CrN/Cr or CrN interlayers, or pre-treated with two-step chemical etching (Murakami's reagent and Caro's acid, MC-treatment).

In particular, growth, morphology, wear endurance and adhesion of the CVD deposited diamond films onto peened CrN/Cr interlayer were looked into. Diamond coatings on peened CrN/Cr interlayers exhibited a rougher surface morphology than as-prepared CrN/Cr films as a result of the surface roughening of the ductile Cr layer produced by the repeated impacts on it of the diamond powders during FBP. FBP was found to be a necessary step in improving the scarce adhesion of CVD diamond onto CrN/Cr-interlayer.

However, the use of FB peened CrN/Cr interlayer did not represent the best way to pre-treat WC-Co substrates, as the unpeened single-layer CrN, or the use of MC pretreatment, was found to ensure better adhesion and wear endurance.

Keywords: Adhesion; Interlayer; Diamond film; Fluidized bed

1. Introduction

Highly stressed components such as high performance cutting tools for heavy duty machining industry demand, in the development and concept phase, an optimal assessment of material, manufacturing process and design, based on tools end-use and actual loading conditions. The material surface always plays a crucial role in the manufacture of high performance cutting tools, as wear or, even worse, macroscopic damages usually starts at the surface caused by the removal or displacement of material by the mechanical action of the lubricated (or not) contacting interface between tool and workpiece.

In general, high performance materials for cutting tools have to accomplish several requirements: i) satisfy the static and dynamic loading requirements; ii) satisfy the requirements in respect to wear; iii) allow easy manufacturing and processing. Such a material that has to fulfil all these demands can, in most case, only be manufactured by material combination or through composite design. Co-cemented tungsten carbide (WC-Co) responds to most of the mentioned requirements and is widely used in the machining, mining and stone cutting industry. However, WC-Co cutting tools are found to wear rapidly at any time the machining of some particular materials such as green ceramics, graphite or metal matrix composite is performed. In this respect, the application of surface overlay coatings to enhance the overall machining effectiveness of WC-Co by reducing the tools down-time, increasing the cutting productivity and improving the quality of the machined surface are becoming more and more attractive.

Diamond films grown by Chemical Vapour Deposition (CVD) are widely used as surface overlay coatings onto WC-Co cutting

* Corresponding author.
E-mail address: barletta@mail.mec.uniroma2.it (M. Barletta).

0925-9635/$ - see front matter © 2008 Published by Elsevier B.V.
doi:10.1016/j.diamond.2007.12.059

tools to improve their wear endurance, thus providing enhanced surface hardness, large thermal conductivity, reduced friction and better corrosion protection, as well. However, diamond-coated tools are useless in case of low adhesion of the surface overlay coating with the underlying substrate. In particular, CVD of adherent diamond films onto WC-Co tools can be very critical if any efforts to minimize the presence of surface cobalt are not produced. In fact, during the initial steps of high temperature diamond deposition process, the leakage of cobalt from the Co-cemented carbide catalyzes the formation of interfacial sp^2-carbon [1]. This weak graphitic layer at the interface results in poor adhesion between the diamond coating and the substrate [2–5]. What is more, at typical diamond CVD temperatures (650–950 °C), carbon is soluble in Co up to 0.2–0.3 wt.% C [6]. Accordingly, diffusion of carbon from the deposited diamond phase into the metal binder may occur in typical CVD growth conditions [7]. Consequently, widespread voids can form at the diamond/substrate interface, thus reducing the interfacial contact area and, consequently, the adhesion strength. Therefore, the deposit of adherent diamond coatings onto WC-Co tools can be effectively performed only after the removal of the surface cobalt.

Several procedures can be distinguished whereby the untreated WC-Co substrates material can be improved: i) the removal of the Co-binder phase from the substrate surface with aqueous solutions of either strong oxy-acids or hydrochloric acid [8–15]; ii) the use of interlayer materials as carbon and cobalt diffusion barrier to suppress interactions of Co with the hydrocarbon radicals rich gas phase in the CVD atmosphere during deposition and, afterwards, with the deposited diamond [13,16–23]; iii) the use of interlayer materials with intermediate thermal expansion coefficient between WC-Co and diamond to relieve the residual thermal stresses [13,19–23]; iv) the heat treatment of as-ground WC-Co to modify the substrate surface morphology and reduce surface Co concentration by decarburization of the external layers of the tungsten carbide, resulting in the formation of an outermost layer of metallic tungsten [24] or the re-sintering of WC-Co substrates in a protective atmosphere [25]; v) the micro-roughening of WC-Co surface morphology by selective attack of the tungsten carbide with Murakami's reagent ($K_3Fe(CN)_6$: KOH: H_2O = 1: 1: 10) [26] or by multiple laser pulses having irradiation densities ranging from 3.0 to 6.0 J/cm^2 [27], with both techniques requiring a further step in which surface Co is chemically etched.

More recently, new procedures based on the use of interlayers and/or mechanical pre-treatments of the WC-Co substrates have been proposed to improve the adhesion between WC-Co and CVD diamond [28–30]: i) the use of PVD-arc CrN coatings as effective interlayers [28]; ii) the micro-roughening of the WC-Co surface morphology by peening at moderate pressure with a fluidized bed of brittle diamond powders joined with the chemical dissolution of surface Co [29]; iii) the micro-roughening of CrN/Cr coated WC-Co substrates at moderate pressure with sand blasting equipment, whereas unpeened CrN/Cr interlayers exhibited inadequate adhesion levels of the superimposed diamond films [30]. Nonetheless, comparative evaluations among the latest pre-treatments used to improve the adhesion of diamond coatings onto WC-Co substrates do still miss. Therefore, establish a ranking among the different procedures would be a crucial issue to overcome in order to better support tools manufacturers in their operative choices.

In this respect, the present study deals with the analysis of CrN/Cr diffusion barrier interlayers deposited onto WC-Co slabs and FB peened by brittle diamond powders prior to diamond CVD. The proposed pre-treatment was compared with the use of unpeened CrN/Cr interlayer, as well as with the well-established two-step chemical etching with Murakami's reagent and Caro's acid [26] and the effective CrN interlayer deposited by PVD-arc technique [28].

FBP of the CrN/Cr interlayer deposited onto WC-Co slabs was found to micro-roughen the ductile outermost Cr-layer as result of the repeated micro-impacts on it of the diamond powders. The impacts also generated small diamond debris, which were in part retained inside the ductile Cr-layer (i.e., embedding phenomenon [28]), thus providing anchors for the following CVD diamond coating. This way, a significant improvement of the adhesion between the diamond film and the underlying layers was promoted by FBP, whereas unpeened CrN/Cr interlayer onto WC-Co substrate led to the almost spontaneous delamination of the diamond film after CVD.

To the contrary, the application of CrN interlayer material and the micro-roughening of WC-Co surface by selective attack of WC with Murakami's reagent followed by chemical dissolution of Co-phase did lead to better adhesion and wear resistance of the CVD diamond film than the use of FB peened CrN/Cr interlayer.

2. Experimental

2.1. Materials

$10 \times 10 \times 3$ mm^3 WC–5.8 wt.% Co as-ground samples (supplied by Fabbrica Italiana Leghe Metalliche Sinterizzate SpA, Anzola d'Ossola, VB, Italy) were used as substrates. The average grain size of the hard metal substrates was 1 μm, Rockwell A hardness was 90.0 HRA and transverse rupture strength (TRS, according to ISO 3327) was 2900 MPa.

2.2. Substrate pre-treatments

2.2.1. PVD-interlayer material

Films of CrN (thickness 7 μm) or CrN/Cr (overall thickness 4 μm) were deposited onto the WC-Co samples using a PVD-arc plant (Microcoat S.p.A., Italy). During the initial stages of PVD deposition, a thin metallic Cr layer (≤200 nm) was deposited on the WC-Co substrates. The CrN/Cr interlayer can be defined as a sort of graded coating. In fact, the bi-layer CrN/Cr was achieved by progressively decreasing the nitrogen concentration inside the deposition chamber from 100% to 0% of the gas phase, and increasing the argon concentration. This way, the resulting CrN layer is progressively poorer in nitrogen going towards the outermost layers. However, when the nitrogen is completely replaced by the argon in the gas phase, a resulting layer of metallic-Cr is superimposed on the underlying graded CrN layer.

2.2.2. Fluidized Bed Peening (FBP)

A recirculating FB, 40×40 mm^2 as cross section and 100 mm as static bed height, of diamond powder (mesh size 120, factor shape 0.67, supplied by Poligem Srl, Italy), working in transport regime (pressure 2 bar), was used as alterative technique to prepare the WC-Co substrates before CVD (Fig. 1). FBP presents significant advantages compared to conventional shot peening as it allows uniform treatments on large surfaces, use of lower operational pressure and longer-lasting media, potential for self-regeneration of the diamond media, continuous and easy-to-automate treatments, relatively reduced cost and processing time, low environmental impact and operational safety [31–32].

Details of the experimental apparatus are elsewhere reported [28]. Here, it is worth remarking that the employed experimental apparatus consists of: i) a fluidization column, 1.2 m long and 2.5 mm thick, made from AISI 304 stainless steel and equipped with glass portholes for inspection; ii) a rotary screw compressor Quincy model QGB 15 maximum powder 15 kW, flow rate 0–130 m^3/h, pressure ranging 0–10 bar used to feed purified air lacking in moisture and oil to the fluidized bed unit; iii) flowmeters, pressure probes, hygrometers and thermocouples to monitor the process and ensure the stability of the fluidization regime.

FBP is based on the fundamental principle of the powder fluidization [29,31]: in this respect, when enough flow rate is supplied to the fluidization column, the diamond powders become individually suspended in the air flow, while on the whole the bed of powder remains motionless relative to the column walls. As the velocity of the gas flowing across the bed is slowly increased, the heterogeneous character of the bed first reaches its peak and then gradually changes. As the transport velocity is approached, a sharp increase of powder carry-over occurs. The dust collection and solid recycle system of the fluidized bed apparatus (Fig. 1) avoids the dispersion into the environment of the elutriated powders, and, this way, a relatively large solid concentration, typical of the fluidized bed in transport regime, can be retained in the fluidization column.

Table 1
The description of the different phases of the deposition processes investigated

	Scenario 1	Scenario 2	Scenario 3	Scenario 4
Stage I	CrN	CrN/Cr	CrN/Cr	Murakami's reagent
Stage II	Seeding	Seeding	FBP	Caro's acid
Stage III	–	–	–	Seeding
Stage IV	8 h CVD	8 h CVD	8 h CVD	8 h CVD

FBP of the CrN/Cr coated WC-Co substrates was performed by entirely dipping them inside the fluidized diamond powders. The substrates were held on the shaft of a direct current electric motor and, being rotated at low speed (i.e., 60 rpm), they were exposed to the repeated impacts of incoming diamond powders (Fig. 1). The assessment of the optimal fluidized bed parameters was achieved by studying the influence of the processing time and pressure on the surface morphology of the outermost metallic Cr layer.

2.2.3. Substrates pre-treatments

Table 1 summarizes the scheduling of the stages involved during the preparation of the as-ground WC-Co before diamond film deposition in order to enhance diamond nucleation, to suppress the deleterious effects of the binder and to increase the contact area at the interface. Following each pre-treatment, the substrates were washed with acetone and de-ionized water in an ultrasonic vessel.

Four different scenarios were investigated. As-ground WC-Co substrates were PVD-coated with CrN (Scenario 1, interlayer thickness 7 μm) and CrN/Cr bi-layer (Scenarios 2 and 3, overall thickness 4 μm). CrN/Cr coated WC-Co substrates (Scenario 3) were then submitted to FBP for 30 s at 2 bar. One more as-ground WC-Co substrate was submitted to two-step chemical etching (MC treatment, Scenario 4). MC is a well-known two-step chemical pre-treatment [26]. Accordingly, the as-ground WC-Co substrate was first etched for 15 min with Murakami's reagent (10 g $K_3[Fe(CN)_6]$ + 10 g KOH + 100 ml of water). Then, it was subjected to further etching with Caro's acid (3 ml 96 wt.% H_2SO_4 + 88 ml 30% w/v H_2O_2) for 10 s.

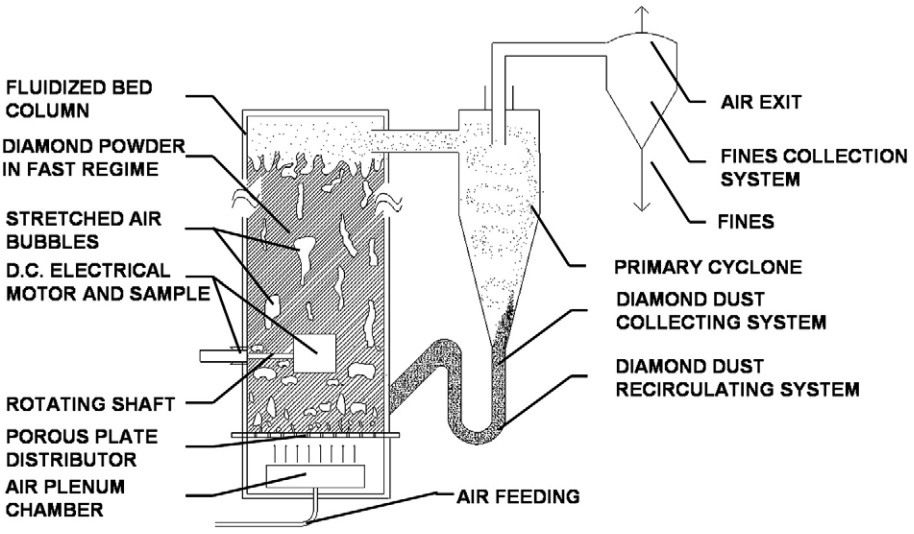

Fig. 1. The FB experimental apparatus.

Prior to diamond deposition, all substrates but the FB peened ones were ultrasonically seeded for 15 min in a 1/4 μm diamond suspension (50 ct/l in absolute ethanol), followed by ultrasonic cleaning in ethanol.

2.3. Chemical vapour deposition

Diamond syntheses were performed in a stainless steel hot-filament chemical vapour deposition (HFCVD) chamber elsewhere described [12]. The gas phase, a mixture of hydrogen and methane with a CH_4/H_2 volume ratio fixed to 1.0%, was activated by a tantalum filament (0.3 mm in diameter) wound in a 1.4 mm internal diameter spiral and positioned at 8 mm from the substrate surface. The filament temperature (2100±50 °C) was monitored by a two-colour pyrometer (Land Infrared model RP 12). The total pressure of the gas mixture in the reactor was 4.8 kPa and flow rate 300 standard cm^3 min^{-1} (sccm). The substrate was placed on a molybdenum ribbon shaped into a rectangular crucible. The substrate temperature (650 °C) was monitored by a Pt/Pt–10%Rh thermocouple pressed against this ribbon at the centre of the sample. Deposition rate, under these CVD conditions, was around 0.5 μm/h. Deposition time was set at 8 h.

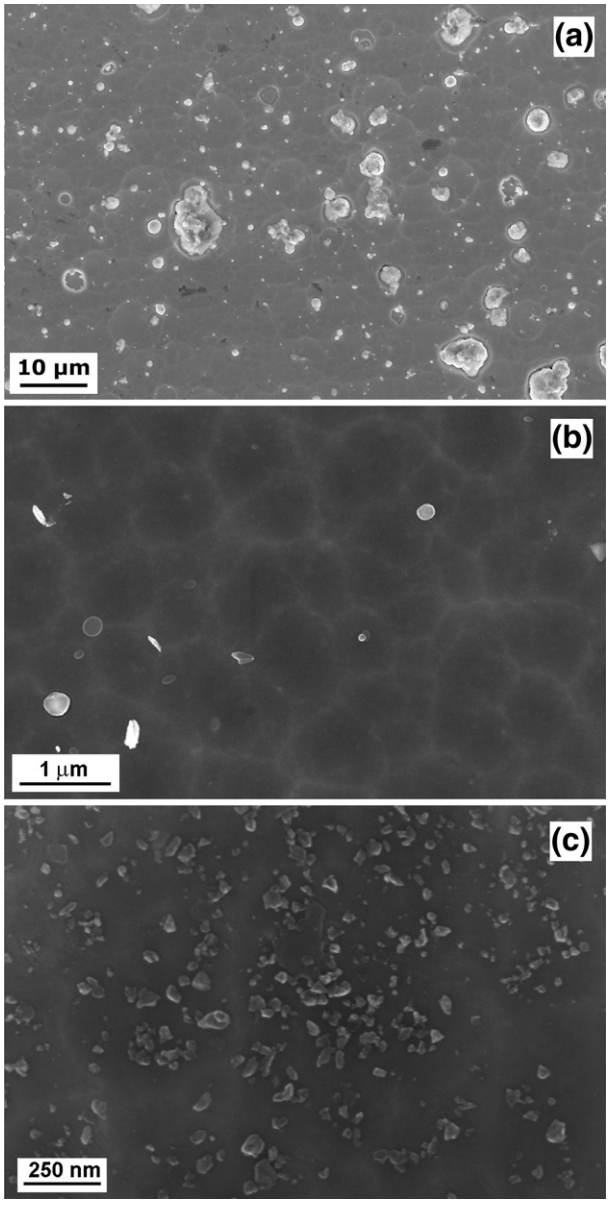

Fig. 2. The morphology of CrN interlayer: (a) overall view; (b) detail on a smooth zone almost without droplets; (c) after seeding with diamond suspension.

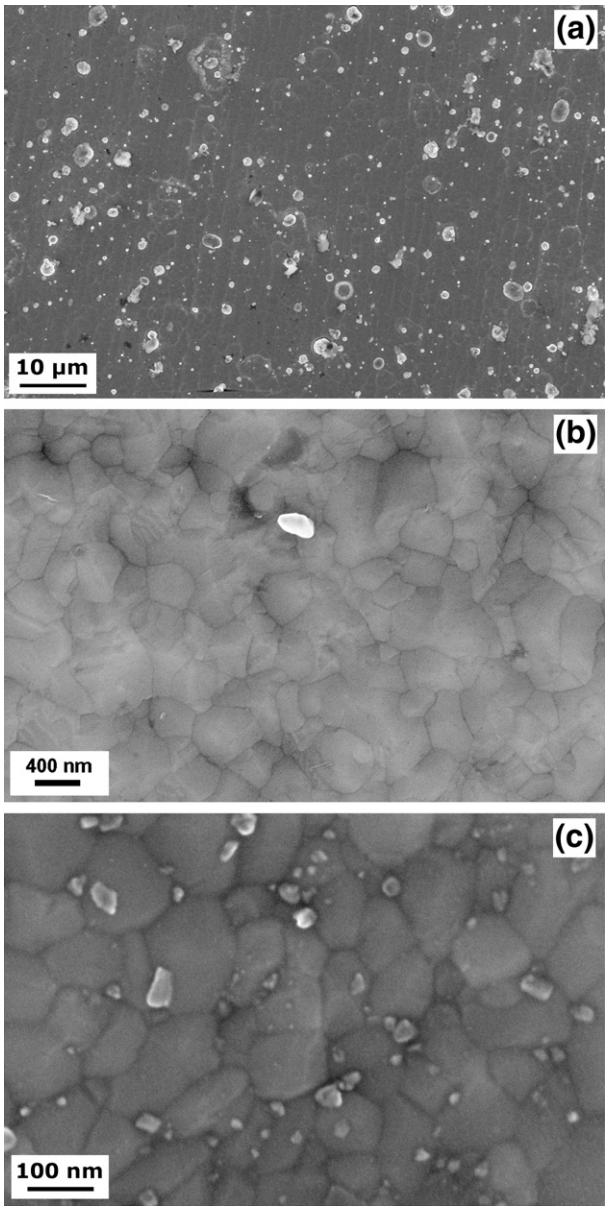

Fig. 3. The morphology of CrN/Cr interlayer: (a) overall view; (b) detail on a smooth zone; (c) after seeding with diamond suspension.

2.4. Characterization tests

PVD interlayers were characterized before and after diamond deposition by $\theta/2\theta$ and grazing incidence ($\omega=1°$) X-Ray Diffraction (XRD) with a Philips X'Pert Pro diffractometer, equipped with a plane mono-chromator using Cu Kα radiation ($\lambda=1.5418$ Å). PVD and CVD films surfaces were observed by Field Emission Gun Scanning Electron Microscopy (FEG-

SEM, LEO model Supra 35) and Energy Dispersive X-Ray Spectroscopy (EDS, Oxford Instruments Ltd., model Inca 300).

The 3D morphology of the PVD and CVD coatings was obtained with a Taylor Hobson Surface Topography System model TalySurf CLI 2000 using the non-contact 300 μm Chromatic Aberration Length (CLA) HE gauge. In comparison to conventional systems, the CLA HE gauge offers superior imaging capability with improved resolution (10 nm and 0.4 μm as vertical and lateral maximum resolution, respectively). Scanning in three dimensions can be performed and the absence of contact between the gauge and the surface being measured ensures the avoidance of any damages to the surface being measured. For the CLA profiler, the samples were located under the gauge and viewed optically, using the high resolution camera built into the Surface Topography System. This enabled the choice of the measurement area and the rough focusing of the gauge. Using the CLA HE scanning mode, a number of patterns (1000), each 4 mm long, was recorded for each sample so as to cover a representative area (16 mm^2) of the entire surface structure. The surface morphology was then examined by using the TalyMap software Release 3.1. As a characteristic of the coatings morphology, standard amplitude, spacing and hybrid parameters for both waviness and roughness profiles (Gaussian filter) were considered.

Dry 'rolling contact' tribological tests were performed by means of an 'ad hoc equipped' static test machine MTS model alliance RT/50 at room temperature to check the diamond film adhesion. Coated samples, kept in a fixed position, were tested at 40 N maximum load (rotating speed: 600 rpm, duration: 30 min) using a WC–9 wt.% Co ball (6 mm diameter). Wear resistance of diamond coatings was assessed by using the non contact profiler. Wear volume, wear track dimensions and average depth of the tracks were obtained by acquiring, for each sample, 1000 points per mm along stylus axis and 1000 roughness profiles per mm along the normal axis. TalyMap software Release 3.1 was used for data analysis and image processing. Repetitions of the tribological tests in different zones of the same sample and on different samples for each investigated scenario ensured the reproducibility of the experimental findings.

3. Results and discussion

3.1. Morphology of the WC-Co substrates after the pre-treatments

Details of the use of CrN interlayers for the deposition of well-adhered diamond films onto WC-Co substrates are reported elsewhere [28]. Here, it is worth remarking that the morphology

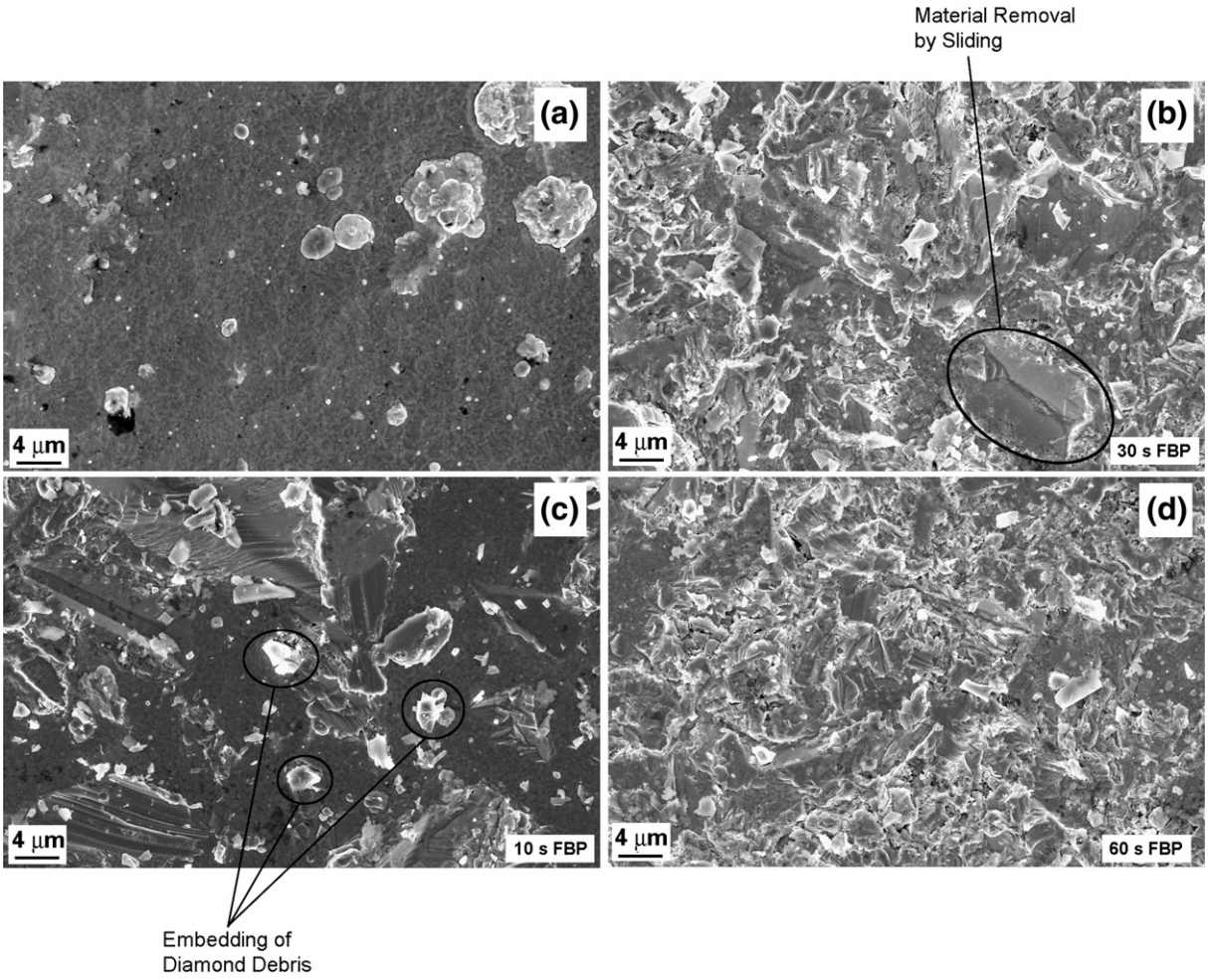

Fig. 4. The morphology of CrN/Cr interlayer after fluidized bed peening (FBP): (a) untreated; (b) 30 s fluidized bed peened; (c) 10 s fluidized bed peened; (d) 60 s fluidized bed peened.

of the CrN film is characterized by the presence of widespread droplets, which seldom are larger than 5–6 μm (Fig. 2a). Details of the smooth zones between the droplets and of the seeds left at the substrate surface after the treatment with diamond suspension are reported in Fig. 2b and c, respectively.

The morphology of the CrN/Cr interlayer is reported in Fig. 3. The presence of a few of small globules dispersed on the surface and the fine-grained structure of the outermost metallic Cr layer are clearly detectable in panels a and b, respectively. Fig. 3c shows the same sample after treatment with diamond suspension, with diamond seeds randomly dispersed all over the interested surface.

FBP treatment of the smooth CrN/Cr film caused the micro-roughening of the ductile metallic-Cr layer (Fig. 4), thus altering the starting film morphology. The evolution of the surface features was very fast. In fact, FB treatments 30 and 60 s long led to very similar visual appearance of the exposed zones (Fig. 4b and d). Fig. 5 reports a sketch of the inferred mechanism with the two types of impact: i) the sliding, typical of high impact speed and angle; and ii) the rolling, typical of low impact speed or angle. Both mechanisms cause the release of most of the incoming diamond powders kinetic energy, which acting as self-regenerating micro-tools tend to effectively machine the metallic Cr layer, thus removing (i.e., micro-cutting) or just displacing (i.e., micro-ploughing) the peened material. The action of the micro-ploughing on the metallic-Cr surface morphology can be easily detected from the examination of the FB peened samples in Fig. 4b–d. A case of material removal by sliding was emphasized on the sample FB peened for 30 s in Fig. 4b.

The impact of the brittle diamond powders on the ductile metallic Cr layer during FBP can also cause their splinter fragmentation and subsequent embedding of diamond debris in the softer metallic-Cr layer. The presence of diamond debris can be noted on the sample FB peened for just 10 s in Fig. 4c, where the surface morphology, not too much modified yet, allows their easy detection. Such 'self-induced' seeding, typical of FBP, can promote the nucleation process during the initial stages of CVD [29] and results in a strong mechanical interlocking between the overlay diamond film and the underlying substrate. Accordingly, the time- and cost-consuming treatment of the substrates with diamond suspension can be avoided.

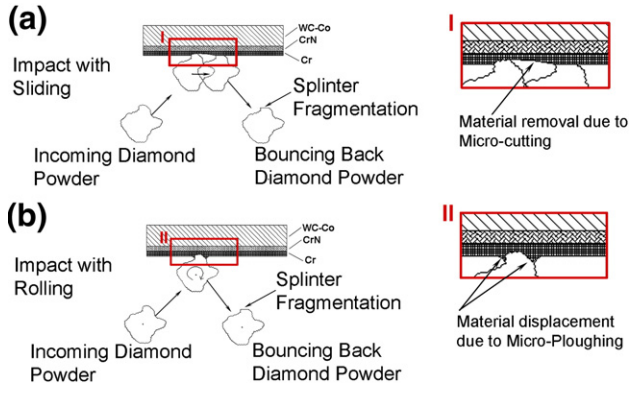

Fig. 5. Mechanism involved in fluidized bed peening (FBP) of CrN/Cr interlayer: (a) sliding; (b) rolling.

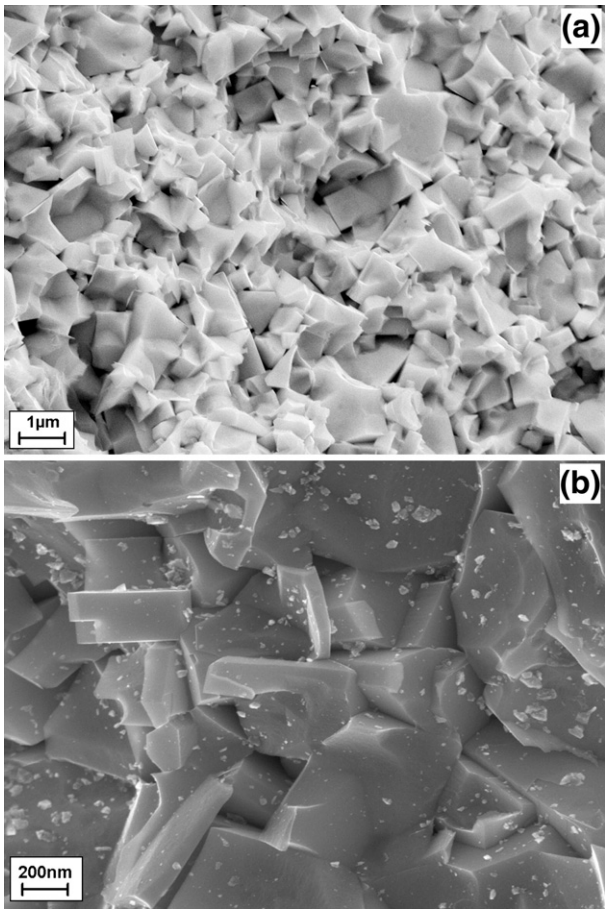

Fig. 6. The morphology of WC-Co substrate after MC treatment: (a) overall view; (b) after seeding with diamond suspension.

Fig. 6a shows the surface morphology of the WC-Co substrate after MC pretreatment. The selective attack to the WC grain of the Murakami's reagent, followed by the surface-Co chemical dissolution by Caro's acid, caused a significant roughening of the WC-Co substrate surface. Fig. 6b shows the same sample after treatment with diamond suspension, with diamond seeds randomly dispersed all over the interested surface.

3.2. Morphology of the WC-Co substrates after CVD

Fig. 7 shows SEM micrographs of diamond coatings deposited onto WC-Co substrates after the different pre-treatments. The presence of droplets due to the PVD-arc CrN/Cr and CrN interlayers is still perceptible in Fig. 7a and c. However, after 8 h CVD, the resulting thicknesses of the diamond films were around 4 μm, thick enough to include part of the droplets.

Diamond coated CrN/Cr interlayers subjected only to seeding prior to CVD were occasionally found to be susceptible of spontaneous delamination of the diamond film on cooling from deposition temperature to room temperature. Fig. 8 shows an image of a full delamination of the diamond coating with a detail showing the carburized contact surface between the underlying interlayer and diamond film (Fig. 8b).

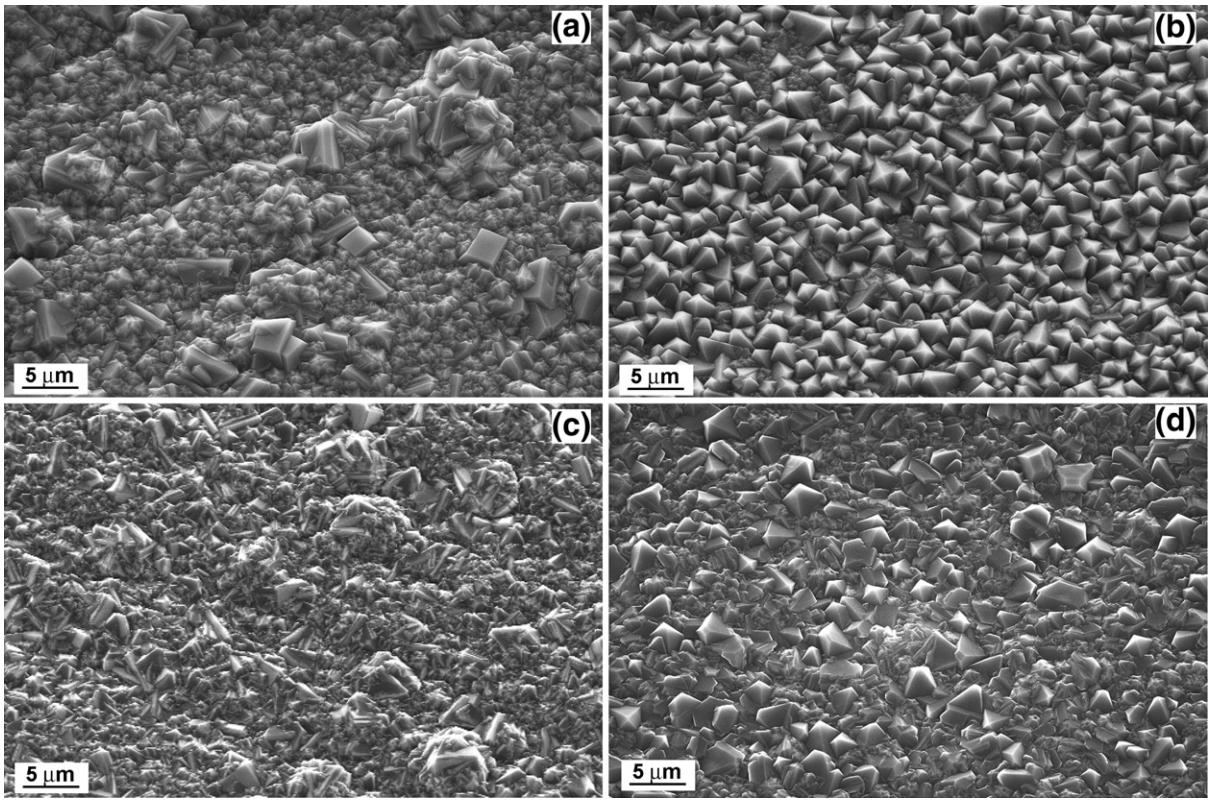

Fig. 7. The morphology of the diamond coatings grown onto: (a) unpeened CrN interlayer; (b) FB peened CrN/Cr interlayer; (c) unpeened CrN/Cr interlayer; (d) WC-Co after MC treatment.

After FBP treatment of the CrN/Cr interlayers, a rougher morphology of the overlaying diamond film should be expected as result of the induced uniform micro-corrugation. By other side, the preferential impacts of the incoming diamond powders on the sticking out droplets should make their removal easier. The resulting surface morphology of the diamond film onto the FB peened CrN/Cr interlayer is mostly smooth and not characterized by the presence of the spiky diamond coated droplets (Fig. 7b). Even after MC treatments, a rougher morphology of the diamond films should be expected, being such procedure found able to induce a marked micro-corrugation of the starting surface morphology of the WC-Co substrate [26]. Nonetheless,

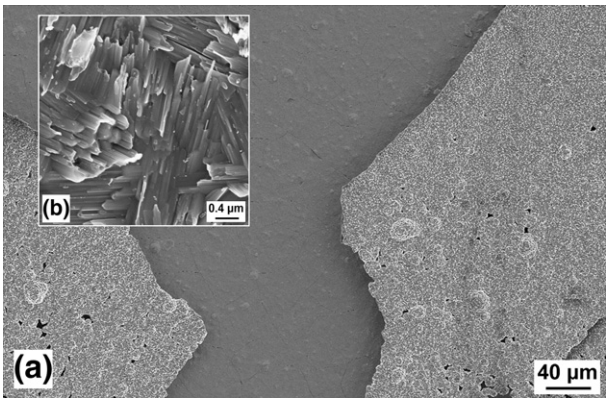

Fig. 8. The delamination of the diamond coatings grown onto unpeened CrN/Cr interlayer: (a) overall view; (b) detail of the carburized Cr-based interlayer.

the roughness parameters in Fig. 9 show that smaller values of amplitude and hybrid parameters characterize the diamond films grown onto WC-Co substrates after the MC and FBP treatments if compared with diamond films grown onto unpeened Cr-based interlayers. This is essentially ascribable to the absence of the spiky droplets, which tend to significantly influence the values of the roughness parameters of the diamond coated unpeened CrN and CrN/Cr interlayers.

The examination of the roughness parameters in Fig. 9 leads to the following further results: *i)* the diamond films grown onto unpeened Cr-based interlayers (Scenarios 1 and 2) are characterized by rough ($R_a \sim 0.42$–0.44 and $R_z \sim 3.36$–3.39 μm, respectively) and spiky surfaces ($R_{\Delta q} \sim 8.9°$ and $R_{Ku} \sim 4.7$–6.5, respectively) due to the presence of the droplets, with the 'bulk of material' below the mean line ($R_{Sk} \sim 0.93$–1.26, respectively); ii) the diamond films grown onto FB peened CrN/Cr interlayer (Scenario 3) presents lower values of the amplitude parameters ($R_a \sim 0.25$ and $R_z \sim 2.1$ μm), yet again with spiky surface ($R_{\Delta q} \sim 6.9°$ and $R_{Ku} \sim 5.9$) due to the heavy FB machining of the ductile metallic-Cr layer and 'bulk of material' below the mean line ($R_{Sk} \sim 0.79$); iii) the diamond film grown onto MC treated WC-Co (Scenario 4) presents the lowest values of the amplitude parameters ($R_a \sim 0.21$ μm and $R_z \sim 1.54$ μm, respectively) and bumpy surfaces ($R_{\Delta q} \sim 6.4°$ and $R_{Ku} \sim 3.27$, respectively) due to the local action of the treatment onto the WC-Co grains, with the 'bulk of material' about the mean line ($R_{Sk} \sim 0$); iv) the lower mean spacing between profile peaks at the mean line shown by the diamond films grown onto FB

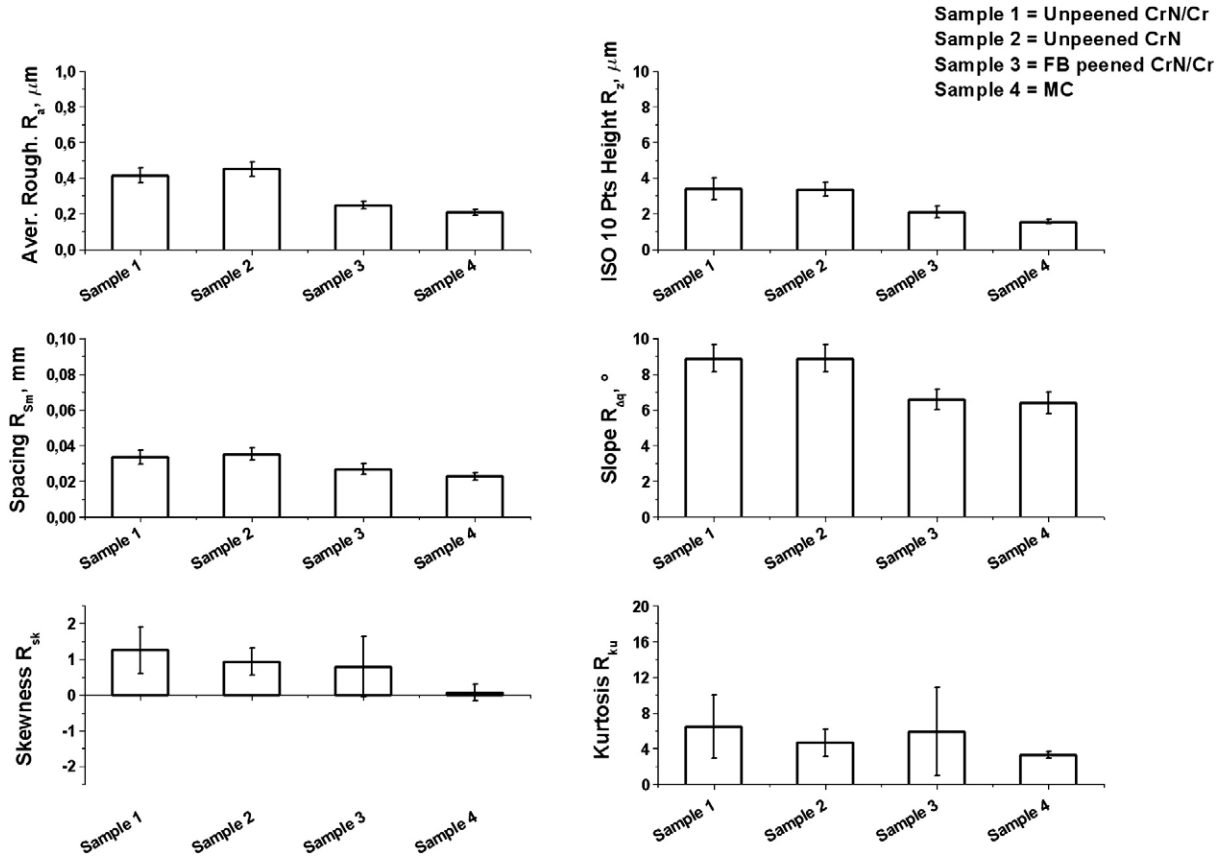

Fig. 9. Roughness parameters of the diamond coatings investigated.

peened CrN/Cr interlayer and MC treated WC-Co substrate (R_{Sm} = 0.22–27 mm) if compared with the diamond films grown onto unpeened Cr-based interlayers (R_{Sm} range 0.36–0.39 mm) witnesses the higher number of peak per unit of length for the substrates deposited under the Scenarios 3 and 4, that is, their uniform micro-corrugated morphology. To the contrary, the last statement confirms how the spiky surfaces, typical of the diamond films grown onto unpeened Cr-based interlayers, result from the superimposition of almost isolated and, occasionally, very large morphological features such as the PVD-induced droplets on an almost flat base morphology.

3.3. Analysis of the CrN–Cr interlayers

Fig. 10 shows the cross section of the diamond coated CrN–Cr interlayer on the WC-Co substrate. As result of the peculiar settings of PVD operational parameters (Section 2.2.1), there is no a well definite interface between the CrN and Cr layers, giving rise to a sort of graded coating. The PVD interlayer becomes progressively poorer in nitrogen concentration moving away from the WC-Co substrate. Finally, the outermost layers of the PVD CrN/Cr coating consist of pure metallic Cr, where the CVD diamond film is subsequently anchored.

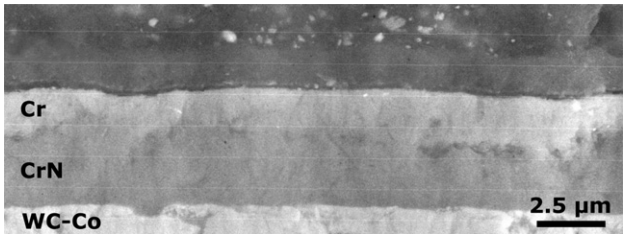

Fig. 10. Cross section of the CrN/Cr interlayer.

Fig. 11 reports the $\theta/2\theta$ and grazing incidence ($\omega = 1°$) X-ray diffraction patterns of the CrN/Cr interlayer before and after CVD deposition. Before CVD deposition, sharp peaks of WC, metallic Cr and the broad CrN (220) peak were detectable in the $\theta/2\theta$ XRD pattern. The grazing incidence XRD pattern showed intense and rather sharp Cr peaks, thus confirming that the outermost layer of the PVD film was composed of metallic chromium.

After CVD, sharp and intense (111) and (220) diamond peaks were present. However, major changes in the interlayer occurred. Metallic Cr peaks were not easily detectable and sharp CrN and Cr_2N peaks in $\theta/2\theta$ XRD pattern were present in addition to very low intensity Cr_3C_2 peaks. Grazing incidence XRD pattern showed Cr_2N peaks and slightly more intense Cr_3C_2 peaks. These results suggest that recrystallization of CrN as well as reactions of Cr with CrN, to form Cr_2N, and carbon species from the gas phase, to form Cr_3C_2, took place. The formation of Cr_2N in diamond coated CrN/Cr PVD films onto WC-Co was the main difference in chemical composition of CrN/Cr and CrN interlayers after diamond CVD. In fact, recent data from our lab and published in the relevant literature [28]

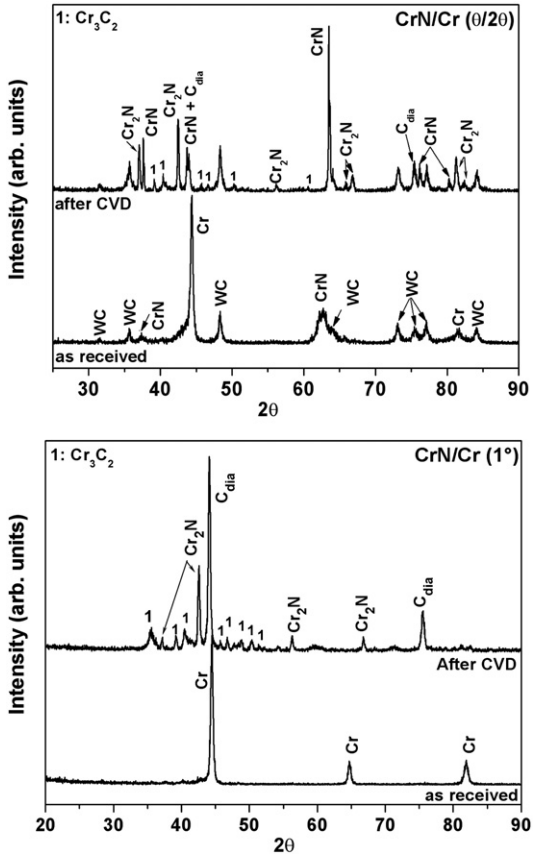

Fig. 11. $\theta/2\theta$ and grazing incidence ($\omega=1°$) XRD patterns of WC-Co substrates with unpeened CrN/Cr interlayer before and after diamond CVD.

did not show the presence of relevant Cr_2N peaks in diamond coated WC-Co substrates using CrN interlayers deposited by the same PVD-arc technique here employed. Those data also showed that the intensity of the Cr_3C_2 peaks, formed on CrN under diamond CVD conditions similar to the ones here employed, was equally low and comparable to the intensity of chromium carbide peaks detected in this work. This fact suggests that a Cr_3C_2 thin layer of similar thickness was formed by reaction of C-containing gaseous precursors with either CrN/Cr or CrN interlayers during CVD.

Fig. 12 reports the grazing incidence XRD patterns of the unpeened and FB peened CrN/Cr interlayer before and after CVD deposition. The comparison of the XRD patterns of the substrates before CVD shows that FBP induced a significant broadening of metallic Cr diffraction peaks, which can be explained by stress induced defects, namely cracking and plastic deformation, caused by the effective machining process [29]. However, FBP of the CrN/Cr interlayer did not influence its modifications occurring during CVD. In fact, the grazing incidence XRD patterns of both unpeened and FB peened samples subjected to 8 h CVD showed sharp Cr_2N and low intensity Cr_3C_2 peaks, and no detectable Cr peaks.

3.4. Tribological tests

Fig. 13 shows the 3D-profilometry of the diamond coated samples after the tribological tests. Despite their spiky surface morphology, diamond coatings grown onto unpeened CrN/Cr interlayer did not withstand the prescribed tribological tests. The first contact of the WC-Co spherical pin on the diamond coatings that remained apparently adherent to the substrate after CVD was always found to cause immediate catastrophic failure (Fig. 13a), that is a sudden delamination of the coating over an extended area. To the contrary, diamond coatings grown onto FB peened CrN/Cr interlayers showed good wear performance. Tribological tests at 20 N load did not leave any damage on the sample surface (Fig. 13b). Tribological tests executed with 30 N and 40 N loads produced a slight (~ 0.1 mm^2 groove surface, $\sim 768{,}000$ μm^3 groove volume) and a quite large groove (~ 0.53 mm^2 groove surface, $\sim 1{,}538{,}000$ μm^3 groove volume), respectively. However, the diamond coatings did not undergo catastrophic failure (Fig. 13c and d). The aforementioned experimental findings state the effectiveness of FBP as preparation technique of the CrN/Cr interlayers before CVD, whilst, in the past, only the machining capability of FBP on bare WC-Co substrate prior to CVD to improve diamond adhesion was ascertained [29].

In particular, the best behaviour of the FBP samples has to be ascribed to the micro-corrugation joined with the spiky surface morphology induced by FBP onto the ductile metallic Cr layer. This time, the micro-corrugation of the CrN/Cr interlayer and the subsequent increase of contact surface between the diamond film and the underlying layers was due to the material removal and/or displacement produced by the impact of the diamond powders during FBP. This morphology is, therefore, quite different from that typical of the unpeened CrN/Cr, whose spikiness is just induced by weakly adhered and sparse large droplets.

The improvement of wear behaviour of diamond coating grown onto peened CrN/Cr interlayer is in agreement with the recent findings by Kumar et al. [30]. They found that the shot peening of Cr/CrN/Cr interlayers did allow to increase the adhesion of the diamond films on WC-Co with respect to unpeened Cr/CrN/Cr. Nonetheless, they missed to compare their coatings with diamond coatings deposited on CrN interlayers or on state-of-art substrates like WC-Co after MC treatment. Indeed, diamond coatings grown onto unpeened CrN

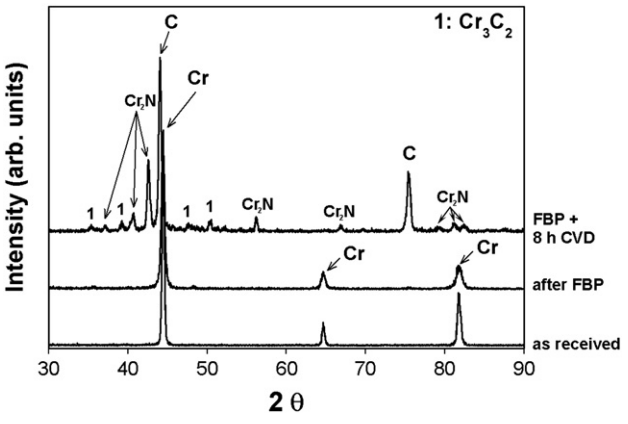

Fig. 12. Grazing incidence ($\omega=1°$) XRD patterns of unpeened and FB peened CrN/Cr interlayer before and after diamond CVD.

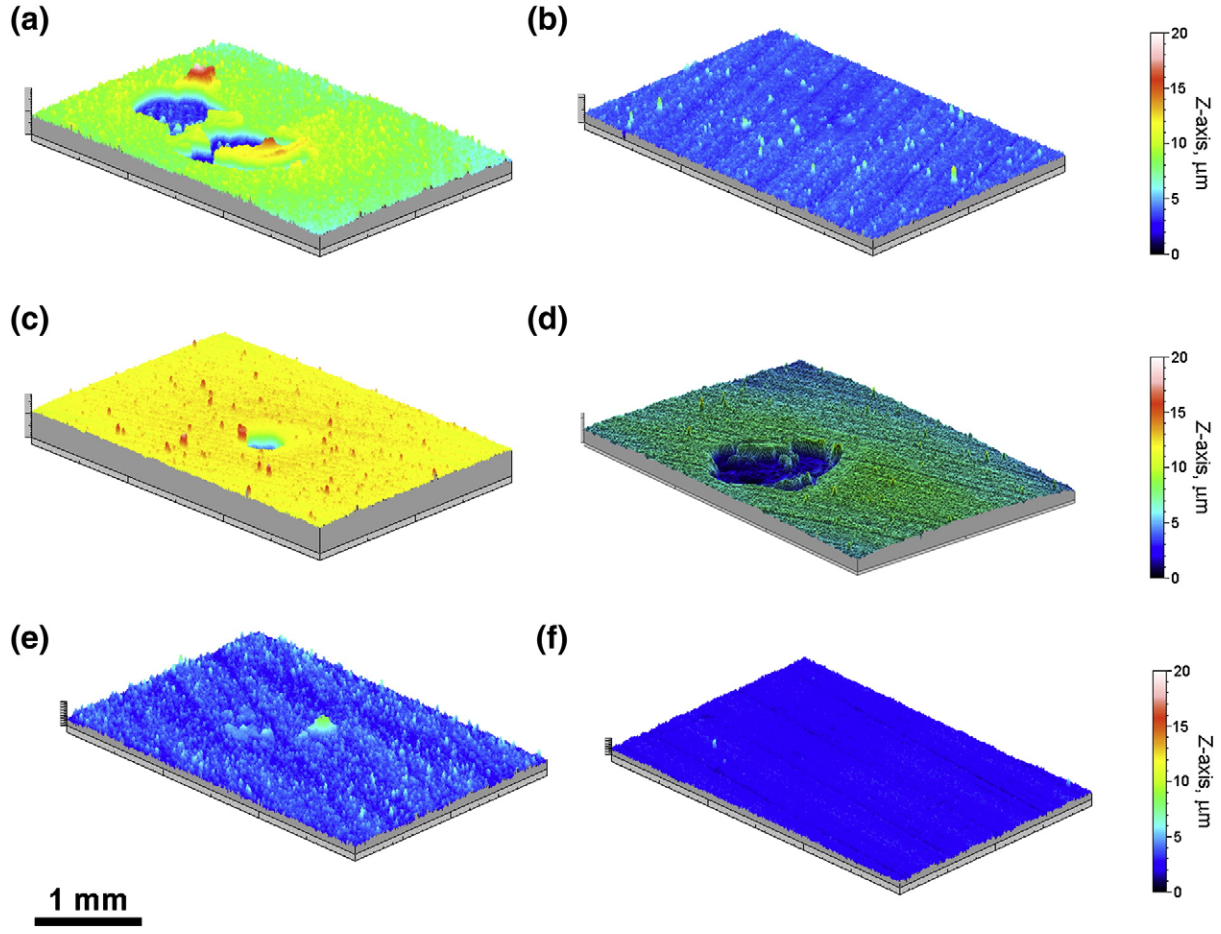

Fig. 13. Tribological test results of the diamond coatings grown onto: (a) unpeened CrN/Cr interlayer at 20 N load; (b) FB peened CrN/Cr interlayer at 20 N load; (c) FB peened CrN/Cr interlayer at 30 N load; (d) FB peened CrN/Cr interlayer at 40 N load; (e) unpeened CrN interlayer at 40 N; (f) diamond coated WC-Co after MC treatment at 40 N.

interlayers as well as onto WC-Co after MC treatment were found to exhibit the best overall behaviour, with no damages being induced from the tribological tests, even at 40 N load (Fig. 13e and f). Diamond coatings grown onto unpeened CrN interlayer tended to retain some material from the WC-Co pin. This may be more likely ascribable to the spiky morphology of such samples due to the presence of large diamond coated droplets on it. Anyway, CrN interlayers were confirmed to be an optimum intermediate layer to increase the wear performance of overlaying diamond coatings, in agreement with what reported in the literature [28].

The large difference in diamond adhesion on unpeened CrN and CrN/Cr interlayers is rather difficult to explain. Their morphologies were found to be quite similar. Moreover, EDS analyses of the delaminated areas of unpeened CrN/Cr substrates did not show any detectable Co. Therefore, the different performance between the two coatings should not be attributable neither to the starting surface morphology of the interlayers nor to the different capabilities of the two PVD coatings as Co diffusion barrier. In the light of previous observations, the different behaviour between the two coatings could be more likely ascribed to the formation of Cr_2N, which was found only in the CrN/Cr interlayers after diamond CVD. Yet again, the different morphology of the chromium carbides, which are formed in CrN/Cr interlayer by reaction of metallic Cr with the activated gas phase in the CVD reactor and in CrN interlayer by reaction of CrN with the activated gas phase in the CVD reactor, can also be supposed to significantly influence adhesion performance of the overlaying diamond films. However, further studies are needed to improve the knowledge of the leading phenomena involved.

Finally, the good wear performance of the diamond coatings grown onto MC treated WC-Co substrates (Fig. 13f) can be ascribed to the effective micro-roughening the pre-treatment was able to induce onto the WC-Co substrates (Fig. 6). This way, very high density of micro-peaks, on which adherent diamond coatings did grow, were evenly distributed all over the WC-Co substrate, guaranteeing high overall wear performance.

4. Conclusion

The effect of different pre-treatments on the adhesion of diamond coatings produced by HFCVD on WC-Co substrates was investigated. It was found that the CrN/Cr PVD interlayers need a roughening treatment prior to CVD in order to achieve satisfactory levels of diamond adhesion. For this purpose a

surface treatment involving a fast fluidized bed (FB) of diamond powders has been used for the first time to modify the staring surface morphology of the CrN/Cr interlayer. FB peened CrN/Cr interlayer films showed good wear resistance of the superimposed diamond films, whereas diamond films deposited on unpeened CrN/Cr interlayer films were not adherent at all. It was also found that as-deposited CrN PVD films allowed to achieve good adhesion levels and wear resistance without any need to modify their roughness even if the surface morphology was very similar to that of as-prepared CrN/Cr interlayers. Accordingly, diamond films deposited on CrN showed excellent wear behaviour characterised by the absence of measurable wear volume after the tribological tests. Diamond coatings grown directly onto WC-Co subjected to two-step chemical etching (MC treatment) showed optimal adhesion and wear resistance, as well. This result can be attributed to a very high density of micro-peaks evenly distributed all over the WC-Co substrate, which promote the growth of adherent and wear resistant diamond coatings.

In the light of experimental results, a rank among the different pre-treatments investigated can be proposed. The best procedures for WC-Co substrates were found to be the use of CrN interlayer and MC treatment. The sole seeding with diamond suspension of CrN/Cr interlayers deposited by PVD-arc technique did not permit to deposit adherent diamond films. FBP improves the capability of CrN/Cr interlayers as intermediate layer between the underlying WC-Co and the overlaying diamond films. Moreover, the diamond fragments embedded in the outermost metallic chromium layer during FBP provided suitable growth centres for diamond in the subsequent CVD process. This fact allowed to avoid a further seeding step with diamond suspension. Nonetheless, wear resistance of the resulting diamond films was found to be lower than diamond coatings grown onto CrN interlayers subjected to a conventional seeding treatment prior to CVD.

Acknowledgments

The authors would like to thank Dr. Roberta Valle (Centro Sviluppo Materiali SpA, Roma, Italy) for PVD depositions and Dr. Gianluca Rubino (Università di Roma 'Tor Vergata', Dipartimento di Ingegneria Meccanica) for tribological tests.

References

[1] X. Chen, J. Narayan, J. Appl. Phys. 74 (1993) 4168.
[2] K. Shibuki, M. Yagi, K. Saijo, S. Takatsu, Surf. Coat. Technol. 36 (1988) 295.
[3] T.H. Huang, C.T. Kuo, C.S. Chang, C.T. Kao, H.Y. Wen, Diam. Relat. Mater. 1 (1992) 594.
[4] F.-M. Pan, J.-L. Chen, T. Chou, T.-S. Lin, L. Chang, J. Vac. Sci. Technol. A 12 (1994) 1519.
[5] A. Inspektor, C.E. Bauer, E.J. Oles, Surf. Coat. Technol. 68–69 (1994) 359.
[6] H. Baker (Ed.), ASM Handbook, Alloy Phase Diagrams, Vol. 3, ASM International, Metals Park, Ohio, USA, 1997.
[7] S. Kubelka, R. Haubner, B. Lux, R. Steiner, G. Stingeder, M. Grasserbauer, Diam. Films Technol. 5 (1995) 105.
[8] J. Oakes, X.X. Pan, R. Haubner, B. Lux, Surf. Coat. Technol. 47 (1991) 600.
[9] M.A. Taher, W.F. Schmidt, W.D. Brown, S. Nasrazaani, H.A. Naseem, A.P. Malshe, Surf. Coat. Technol. 86/87 (1996) 678.
[10] A.K. Mehlmann, A. Fayer, S.F. Dirnfeld, Y. Avigal, R. Porath, A. Kochman, Diam. Relat. Mater. 2 (1993) 317.
[11] P.X. Ling, G.Z. Ping, Thin Solid Films 239 (1994) 47.
[12] C. Tsai, J.C. Nelson, W.W. Gerberich, J.J. Herbelein, E. Pfender, Diam. Relat. Mater. 2 (1993) 617.
[13] F. Deuerler, H. van den Berg, R. Tabersky, A. Freundlieb, M. Pies, V. Buck, Diam. Relat. Mater. 5 (1996) 1478.
[14] C.R. Lin, C.T. Kuo, R.M. Chang, Thin Solid Films 308– 309 (1997) 273.
[15] N. Kikuchi, T. Komatsu, H. Yamashita, H. Yoshimura, US Patent 4,731,296 (1988).
[16] I. Endler, A. Leonhardt, H.-J. Scheibe, R. Born, Diam. Relat. Mater. 5 (1996) 299.
[17] M. Nesladek, J. Spinnewyn, C. Asinari, R. Lebout, R. Lorent, Diam. Relat. Mater. 3 (1993) 98.
[18] E. Cappelli, F. Pinzari, P. Ascarelli, G. Righini, Diam. Relat. Mater. 5 (1996) 292.
[19] C.R. Lin, C.T. Kuo, R.M. Chan, Diam. Relat. Mater. 7 (1998) 1628.
[20] W.D. Fan, X. Chen, K. Jagannadham, J. Narayan, J. Mater. Res. 9 (1994) 2850.
[21] J.K. Wright, R.L. Williamson, K.J. Maggs, Mater. Sci. Eng., A Struct. Mater.: Prop. Microstruct. Process. 187 (1994) 87.
[22] S. Silva, V.P. Mammana, M.C. Salvadori, O.R. Monteiro, I.G. Brown, Diam. Relat. Mater. 8 (1999) 1913.
[23] C. Faure, W. Han¨ni, C. Julia Schmutz, M. Gervanoni, Diam. Relat. Mater. 8 (1999) 830.
[24] K. Saijo, M. Yagi, K. Shibuki, S. Takatsu, Surf. Coat. Technol. 47 (1991) 646.
[25] E.J. Oles, A. Inspektor, C.E. Bauer, Diam. Relat. Mater. 5 (1996) 617.
[26] M.G. Peters, R.H. Cummings, European Patent 0519587 A1 (1992).
[27] R.V. Singh, D.R. Gilbert, J. Fitz-Gerald, S. Harkness, D.G. Lee, Science 272 (1996) 396.
[28] R. Polini, F. Pighetti Mantini, M. Barletta, R. Valle, F. Casadei, Diam. Relat. Mater. 15 (2006) 1284.
[29] R. Polini, M. Barletta, M. Delogu, Thin Solid Films 515 (2005) 87.
[30] Z. Xu, L. Lev, M. Lukitsch, A. Kumar, Diam. Relat. Mater. 16 (2007) 461.
[31] J.F. Davidson, R. Clift, D. Harrison, Fluidization, Academic Press, 1985.
[32] M. Barletta, G. Costanza, R. Polini, Thin Solid Films 515 (2006) 141.